Scale-to-scale Energy and Enstrophy Fluxes of Atmospheric Motions via CFOSAT

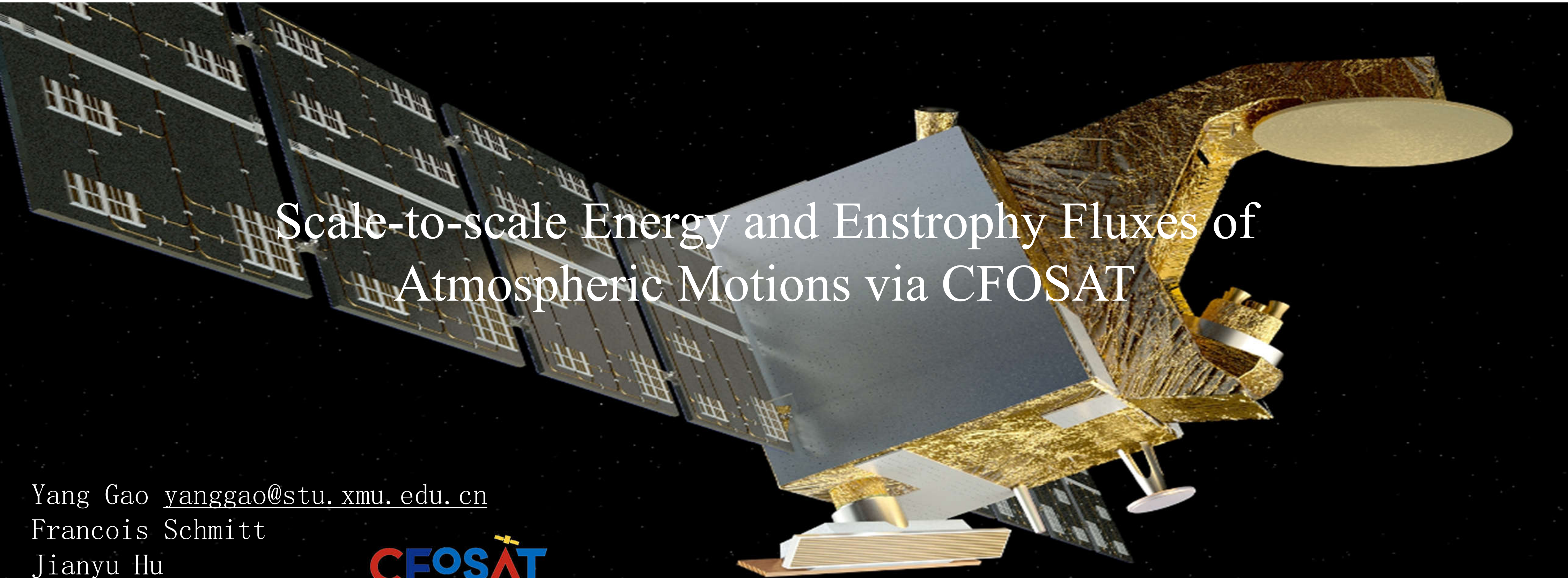

Yang Gao yanggao@stu.xmu.edu.cn
Francois Schmitt
Jianyu Hu
Yongxiang Huang

Content

1、Background

The story begins with a poem written by Richardson (1922).

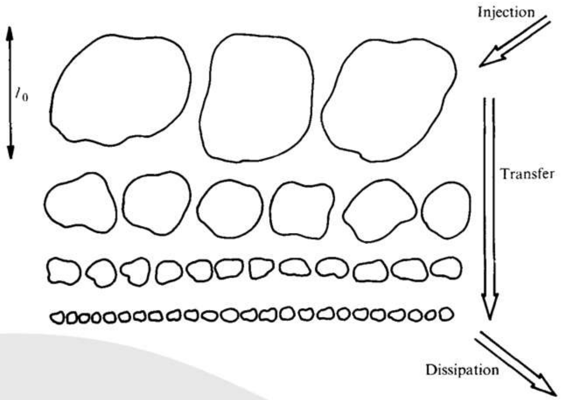

Richardson's cascade theory of turbulence (U. Frisch et al., 1978).

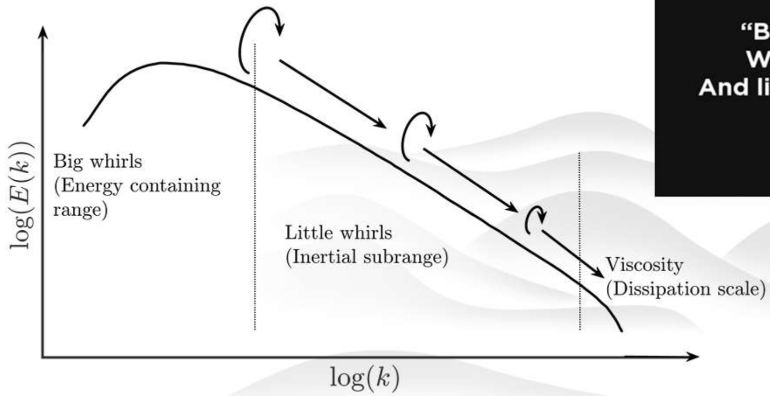

Illustration of energy cascade in a turbulent system.

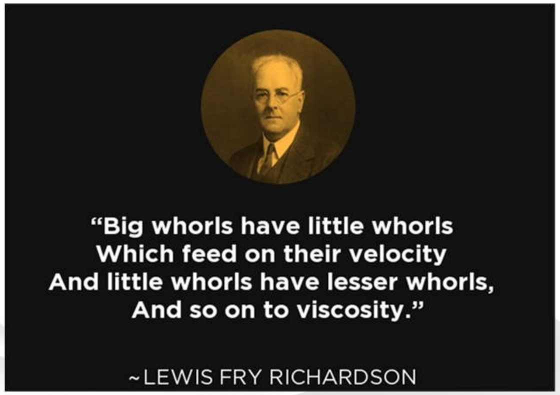

external forcing

dissipation

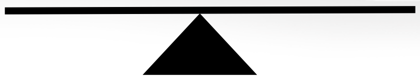

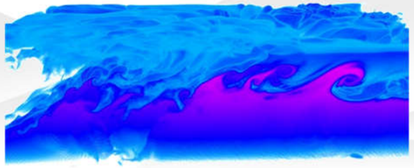

stratification

large aspect ratio

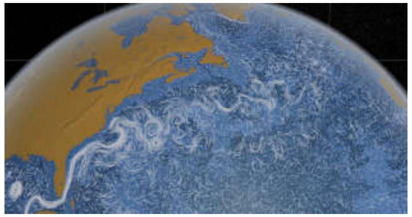

ocean front, current and eddies

The exact balance and the cascade processes are still unknown.

Richardson, L. R. (1922) Cambridge University Press
U. Frisch et al., (1978) J. Fluid Mech.

*Figures adopted from web

1、Background

(a)、Atmospheric motions play key role in the exchanges of energy from place to place in different scales.

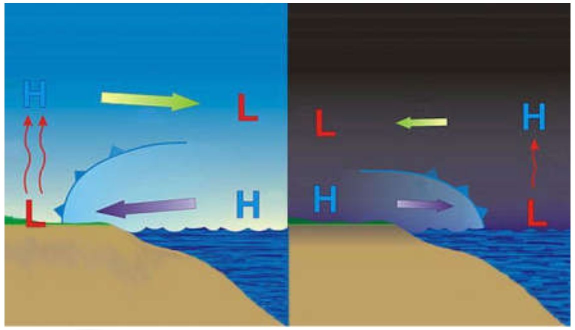

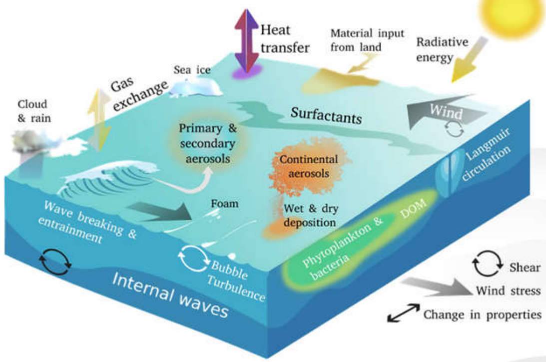

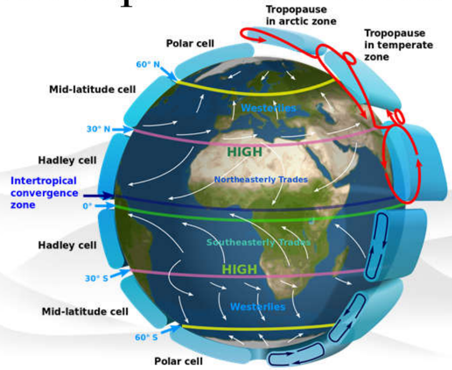

(b)、The factual scale-to-scale energy or enstrophy fluxes are still unknowing due to the lack of high quality data and efficient methods.

Data: The data should have high quality and also cover a wide range of scales.
Methods:

Third-order Structure Functions	**Spectral Approach**	**Filter-Space-Technique (FST)**
Derived from NS Eqs ✓	Derived from NS Eqs ✓	Derived from NS Eqs ✓
Easy to implement ✓	FFT-based ✓	Heavy compute cost ✓
Knowing balance ✗	Regular domains ✗	Partially continued data ✓

Local information can be preserved

Leonard, A. (1975) Adv. Geophys.; Alexakis, A., & Biferale, L. (2018) Phys. Rep.

*Figures adopted from web

2、Data

China France Oceanography Satellite (CFOSAT) observed 12.5 km resolution wind field are used.

The wind are collected by a rotating fan beam scatterometer, with the width of swath equals to 1,000 km.

Data period: December, 2018 to March, 2022.

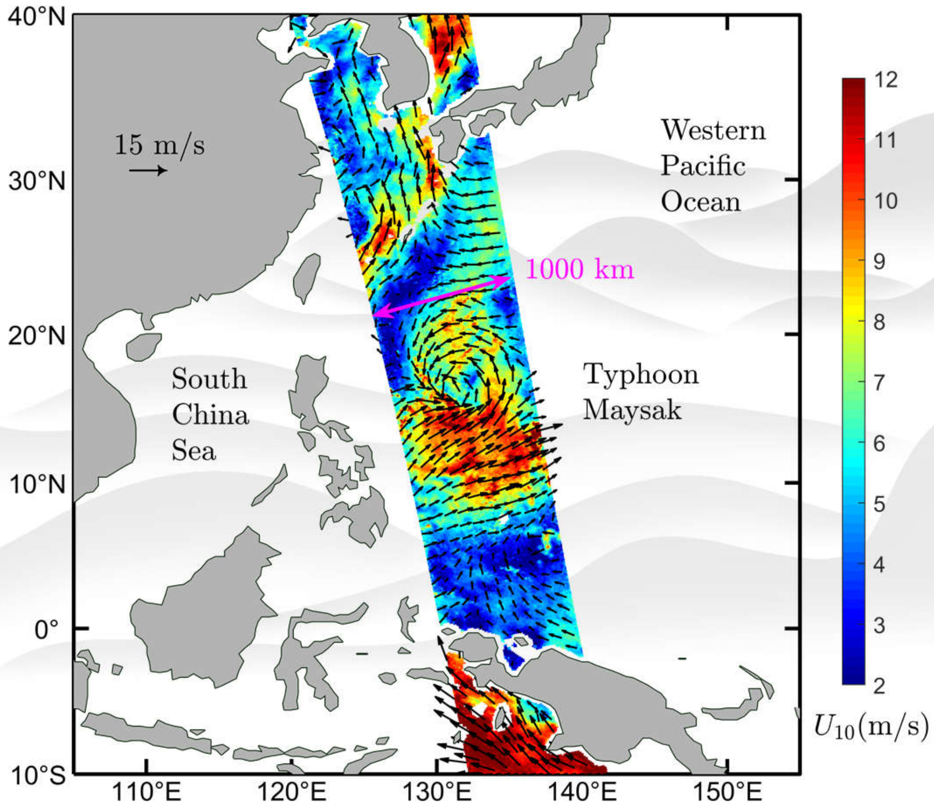

CFOSAT observed wind vectors (black arrows) in the Pacific Ocean on August 27, 2020 during the Typhoon Maysak.

Xu et al. (2019) Acta Oceanol. Sin
Gao et al. (2021) J. Geophys. Res. Oceans

3、Method Filter-Space-Technique (FST, Large-Eddy-Simulation)

$$\Pi_E^{[r]}(x,t) = -\sum_{i,j=1,2}\left[\left(u_i u_j\right)^{[r]} - \left(u_i^{[r]} u_j^{[r]}\right)\right]\frac{\partial u_i^{[r]}}{\partial x_j}$$

Π_E energy flux

$$\Pi_\Omega^{[r]}(x,t) = -\sum_{i,j=1,2}\left[\left(u_i \omega\right)^{[r]} - \left(u_i^{[r]} \omega^{[r]}\right)\right]\frac{\partial \omega^{[r]}}{\partial x_j}$$

Π_Ω enstrophy flux

$\Pi^{[r]}>0$ Forward cascade

$\Pi^{[r]}<0$ Inverse cascade

Where u_i, u_j are the velocity components, ω is the vorticity, which defined as $\nabla \boldsymbol{u}$.

- ☑ The local information of the fluxes are preserved.
- ☑ FST is mathematically exact, it can be generally used without the assumption of homogeneity or isotropy.
- ☑ The data contain gaps and with irregular boundaries can be handled with FST.

Germano, M. (1991) J. Fluid Mech.
Dong, S. , Huang, Y., et al. (2020) J. Fluid Mech

4、Results Global view

Set the filter scale as 250 km

Evident spatial and temporal variations are found

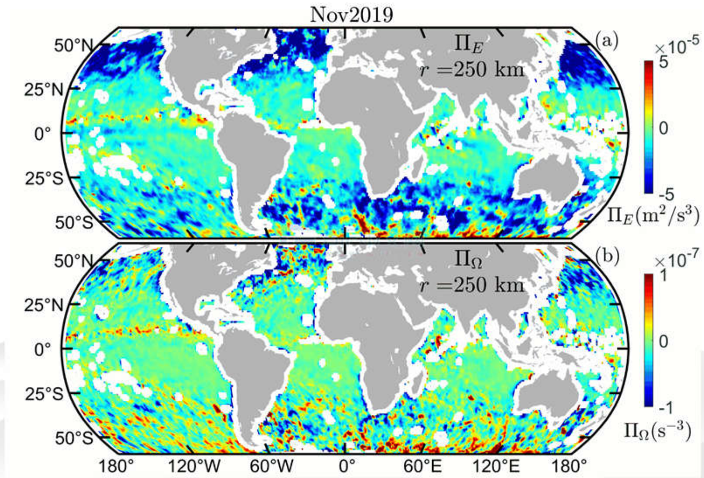

Monthly evolution of (a) energy flux and (b) enstrophy flux.

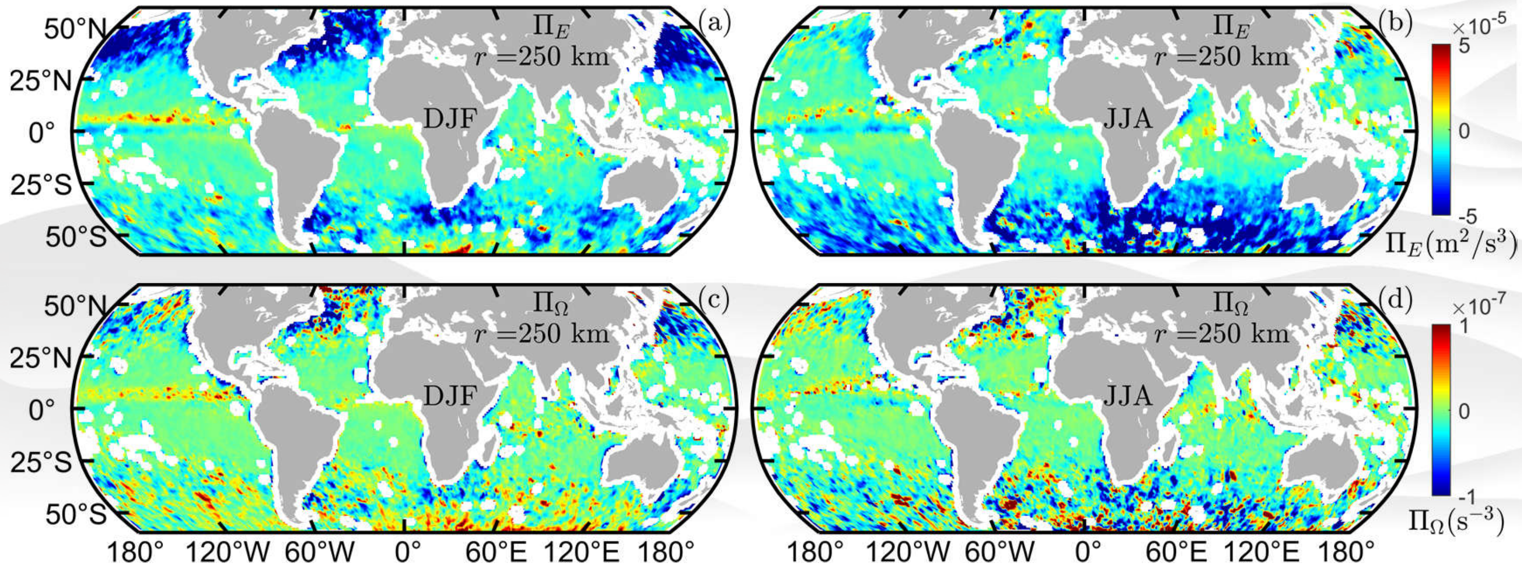

The global distributions of the seasonal averaged energy flux for CFOSAT WS in (a) winter (DJF), and (b) summer (JJA). (c) and (d) are the same, but for enstrophy flux. The filter scale is set as 250 km.

The Π_E and Π_Ω are stronger in winter than the ones in summer.

The Π_E and Π_Ω are stronger in mid-latitudes than the ones in low-latitudes.

Gao et al. under preparation

4、Results Meridional variation

Longitudinal average of the measured fluxes

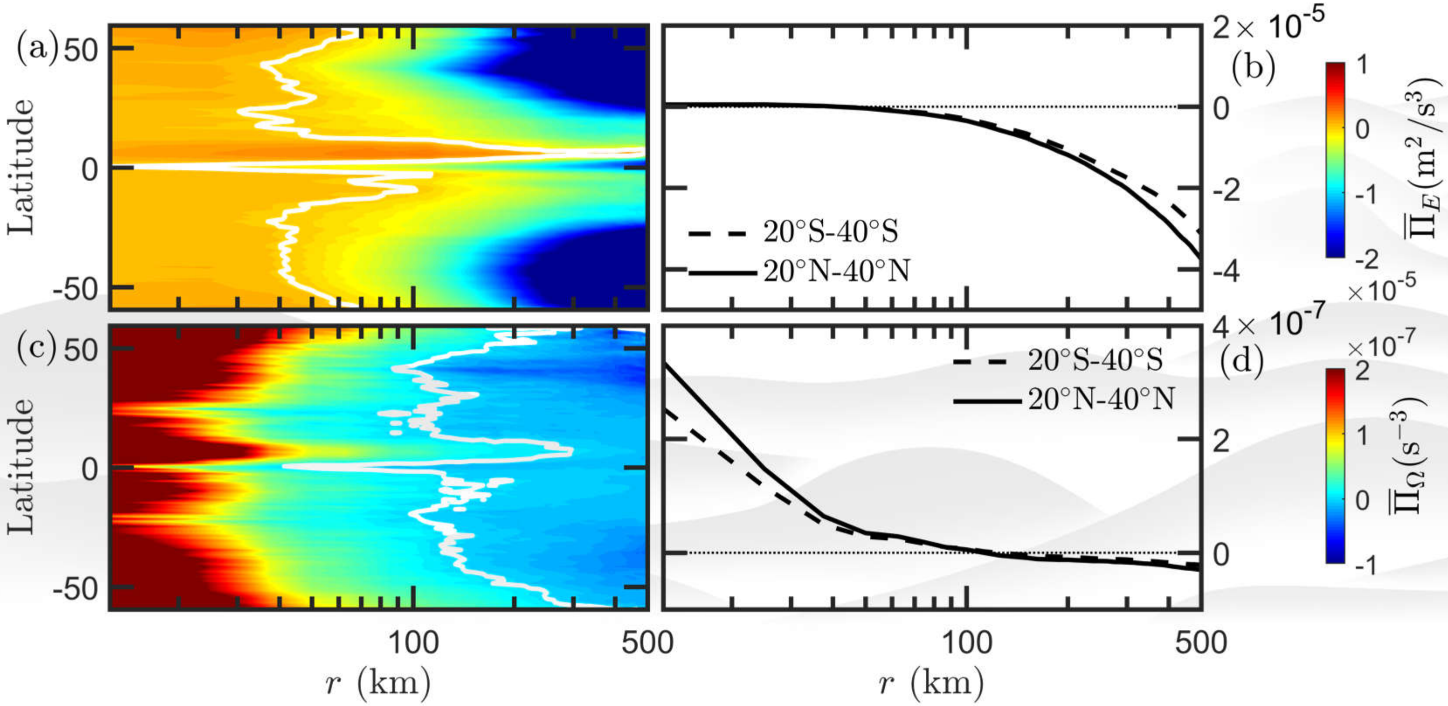

Longitudinal averaged (a) energy flux and (c) enstrophy flux at various scales. The white curves are the contour lines with the value of 0. (b) and (d) are the ensemble averaged energy flux and enstrophy flux curves in two latitudinal ranges, the dotted line is given as a reference with the values of 0.

Meridional variations for Π_E and Π_Ω are found with hemispherical symmetric features.

The values of flux are positive and negative in small and large scales, respectively.

In the selected regions, the transition scales for Π_E and Π_Ω are around 40 km and 100 km, respectively.

4、**Results** Monthly evolution

Monthly average of the measured fluxes

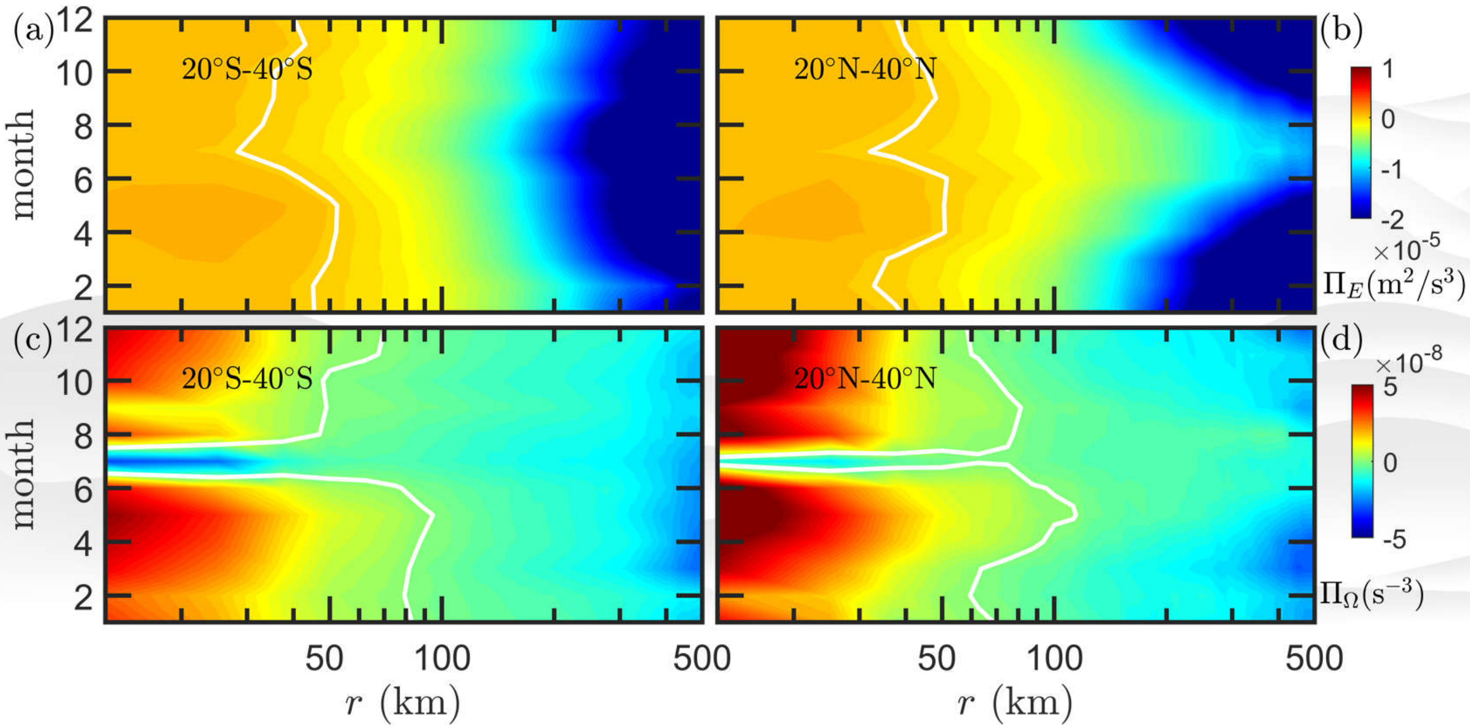

Monthly evolution for multiscale energy flux in the latitudinal ranges of (a) 20°S-40°S, and (b) 20°N-40°N. The white curves are the contour lines with the value of 0. (c) and (d) are the same, but for enstrophy flux.

Monthly variations for Π_E and Π_Ω are found with hemispherical symmetric features.

The Π_E and Π_Ω are stronger in winter than the ones in summer.

5、Conclusion

Meridional and seasonal variations for the energy and enstrophy fluxes are obtained with FST in the scales from 12.5-500 km.

1) Positive and negative energy fluxes are found in the scales less and above 40 km, respectively.

2) Positive and negative enstrophy fluxes are found in the scales less and above 100 km, respectively.

3) Stronger fluxes are occurred in mid-latitudes than the ones in tropical areas.

4) The fluxes in boreal winter are stronger than the ones in summer.

6、Acknowledgments

Funding of the cotutella doctoral research project by Région Hauts-de-France, the CNES (French space agency) TOSCA program, the National Natural Science Foundation of China, the team of China France Oceanography Satellite are acknowledged.